

Effects of temperature on particle trajectories inside hard disk drives

Guoqing Zhang¹ · Yuwen Zhu¹ · Hui Li¹  · Shengnan Shen¹ · Yun Yang¹ · Yibo Chen¹ · Wenbin Sun¹ · Shijing Wu¹

Received: 1 July 2016 / Accepted: 22 November 2016 / Published online: 24 November 2016
© Springer-Verlag Berlin Heidelberg 2016

Abstract The presence of particles, which can intrude into the gas bearing, is one of the most common factors in the failure of hard disk drives (HDDs). Previous works investigated particle trajectories inside air-filled drives without considering temperature effects on the distribution of particles. Actually, especially for the submicron particle, particle trajectories and trapping status are affected by the temperature gradient since the thermophoretic force cannot be ignored. In this paper, considering major heat generation components such as the spindle motor and voice coil motor (VCM), trajectories and trapping status for Al₂O₃ particles inside a 2.5 inch helium-filled drive are simulated by the commercial computational fluid dynamics solver FLUENT with user-defined functions (UDFs). The trapping criterion for Al₂O₃ particles is used as boundary conditions for different colliding surfaces. The results reveal that particles in the air-filled drive will more likely degrade the head–disk interface (HDI) reliability. In addition, after considering the temperature, the particle trapping rate by the disk decreases both inside the air-filled drive and the helium-filled drive. And its reduction inside the air-filled drive is larger. Moreover, small particles will more likely degrade the HDI reliability since they can follow the rotatory flow well and have more chance to collide with the disk surface, and then easily attach onto the disk surface.

1 Introduction

The areal recording density of hard disk drives (HDDs) increases with the decreasing flying height. However, the ultra-low flying height can increase the possibility of contact between the head and disk, which results in the disk surface damage and generates wear particles. The presence of particles, which can intrude into the gas bearing, is one of most common factors in the failure of HDDs.

Some previous works have been focused on particle transport in the head–disk interface (HDI) (Liu et al. 2015, 2016; Cui et al. 2016). Recently, Liu et al. (2011, 2013) investigated particle trajectories in a 2.5 inch air-filled hard disk drive. Their investigations reveal that the majority of particles are trapped by the cover with the assumption that only the cover and filter are set as ideal trapping and reflecting boundary conditions of surfaces regardless of particle velocity. Actually, only the colliding particle with insufficient energy to escape the potential well will be trapped by the surface (Dahneke 1971). Therefore, we proposed a new boundary condition with a velocity based trapping criterion, rather than the simplified assumption of ideal trapping boundaries in our previous work (Zhang et al. 2016a). It simulated trajectories of Al₂O₃ particles in a 2.5-inch HDD, taking into account the trapping criterion. In this simulation, the incident normal critical velocities for Al₂O₃ particles were developed as boundary conditions for colliding surfaces inside the drive. According to Tan's experiment (Tan et al. 2011), the maximum temperature inside the drive can be more than 45 °C at the normal operation. Therefore, the thermophoretic force will obviously affect particle trajectories and cannot be ignored especially for the submicron particle (Stratmann et al. 1988). Yet till now, there are no simulation works on investigating particle trajectories in helium-filled HDDs.

✉ Hui Li
li_hui@whu.edu.cn

¹ Research Center of Electronic Manufacturing and Packaging Integration, School of Power and Mechanical Engineering, Wuhan University, Wuhan 430072, China

This work will investigate particle trajectories by considering major heat generation components such as the spindle motor and voice coil motor (VCM) inside the helium-filled HDD. The trapping criterion of the incident normal critical velocity for Al_2O_3 particles is used as boundary conditions for different colliding surfaces inside the drive (Zhang et al. 2016a). Trajectories for Al_2O_3 particles inside drives are simulated by the FLUENT with user-defined functions (UDFs).

2 Methodology

The equation for the particle motion in a temperature field is described by the Newton's second law:

$$m \frac{dV_p}{dt} = F_{\text{gravity}} + F_{\text{drag}} + F_{\text{saffman}} + F_T \quad (1)$$

where m is the particle mass, V_p is the particle velocity and t is time. Four forces acting on the particle are considered. F_{gravity} , F_{drag} , F_{saffman} , F_T are the gravity force, drag force and Saffman force and thermophoretic force, respectively. Other forces are neglected (Liu et al. 2013).

A geometrical model of a 2.5 inch HDD built in our previous work (Zhang et al. 2016a, b, c, d) is shown in Fig. 1. The model consists of the HGA, actuator arm, VCM, bobbin, magnet, spindle motor, disk, filter, cover, and base. The rotational speed of the disk is 5400 revolutions per minute (RPM). Investigated filling gasses in the HDD include the air or helium and their physical properties at 300 K ambient temperature and 1 atm ambient pressure are listed in Table 1. The heat of the spindle motor and VCM coil are 1.00 and 0.06 W, respectively when the HDD is assumed to be a normal operation. Thermal boundary conditions of inner surfaces of the HDD are set as the coupled heat transfer, while those of outer surfaces include a free stream temperature of 300 K and convection heat transfer coefficient of $9.5 \text{ W/m}^2 \text{ K}$ (Yang et al. 2010). The initial temperature is 300 K in this simulation. The temperature pattern can be obtained by the fluid–structure–thermal coupling simulation. The diameter and density of Al_2O_3 particles used in this work are listed in Table 2.

HDD surfaces are assumed to be polished. Incident normal critical velocities of Al_2O_3 particle are calculated in our previous work. The filter is simplified as wall boundaries and the trapping criterion is applied to all inner surfaces of the investigated HDD except that the filter is set as the ideal trapping boundary (Zhang et al. 2016a). The UDF DEFINE_DPM_BC is used to specify user-defined boundary conditions for particles. In addition, the UDF PARTICLE_STATISTICS is developed to determine particles' final trapping positions.

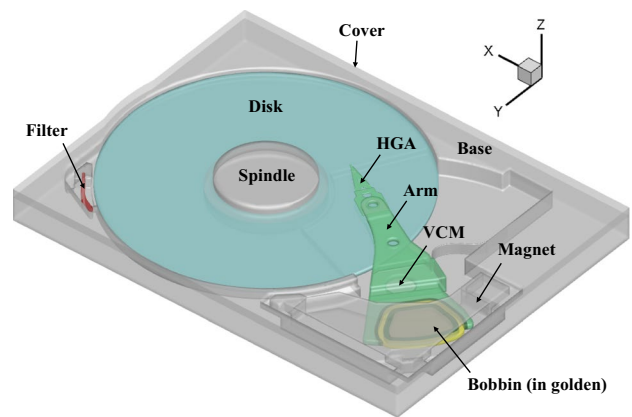


Fig. 1 Geometrical model of a 2.5-inch HDD

Table 1 Physical properties of the air and helium used in this work

Properties	Air	Helium
Density: ρ (kg/m^3)	1.251	0.179
Thermal conductivity: K ($\text{W/m}\cdot\text{K}$)	0.024	0.1513
Specific heat: C_p ($\text{J/kg}\cdot\text{K}$)	1007	5193

3 Results and discussion

3.1 Characteristics of fluid field

Figure 2 shows a top view of the temperature distribution. It can be found that the maximum temperature of the VCM coil inside the air and helium-filled drive is 325.8 and 312.8 K, respectively. The average temperature of the disk surface inside the helium-filled drive is 5 K lower than that of the air-filled drive. It indicates that the helium-filled drive has a higher heat stability due to its larger thermal conductivity and specific heat compared to the air as listed in Table 1.

Figure 3 provides the velocity distribution at the plane of $Y = 0 \text{ mm}$. It can be seen that the velocity along the vertical direction inside the helium-filled drive changes more smoothly compared with the air-filled drive. With the disk rotating at 5400 RPM, the transition Reynolds number of the disk with a 65 mm diameter in the 2.5 inch drive is 80,152 for the air and 6548 for the helium, respectively. Since the transition Reynolds number from the laminar flow to turbulent flow is 2×10^4 (Ng et al. 2011), the flow inside the air-filled drive is turbulent, and that is laminar inside the helium-filled drive in this work.

Table 2 The diameter and density of Al_2O_3 particles

Material	Density: ρ_p (kg/m^3)	Diameter: d_p (μm)
Al_2O_3	3970	0.3, 1, 5, 10

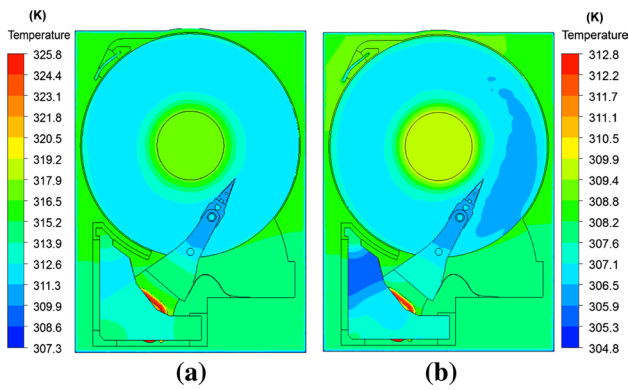


Fig. 2 Temperature distribution inside the **a** air-filled and **b** helium-filled drive

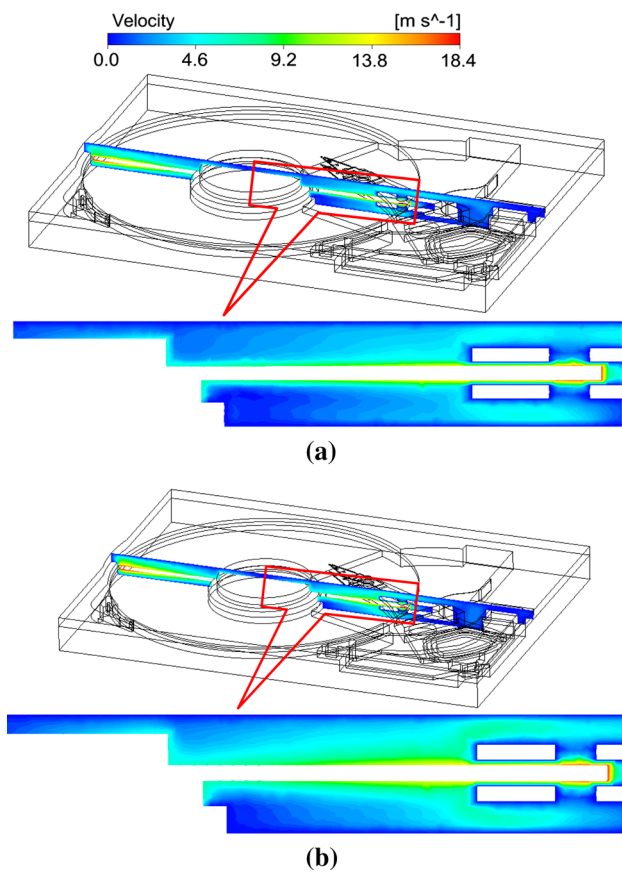


Fig. 3 Velocity distribution inside the **a** air-filled and **b** helium-filled drive at the plane of $Y = 0$ mm

Figure 4 shows the temperature gradient contour inside air- and helium-filled drives. It can be seen that the temperature gradient at the inner diameter (ID) (as marked by the black dashed circle) is higher than in other areas inside the two types of drives. One of the reasons is that the spindle

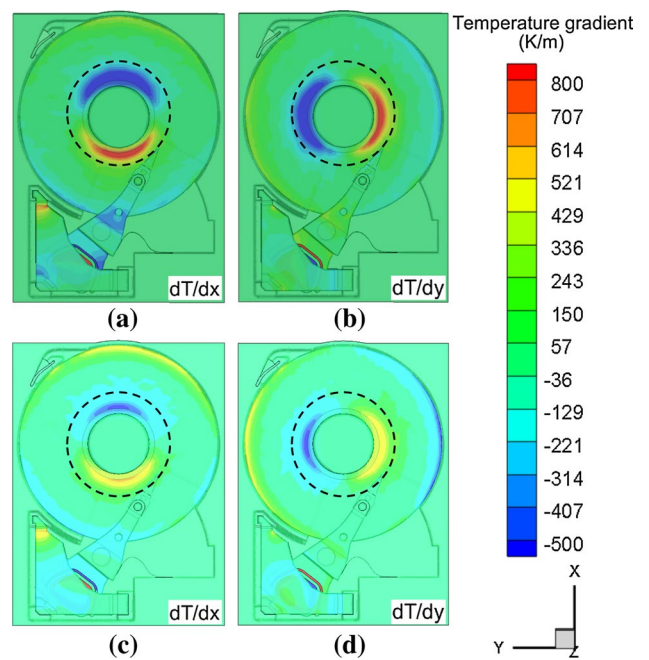


Fig. 4 Temperature gradient in **a, b** air-filled and **c, d** helium-filled drives

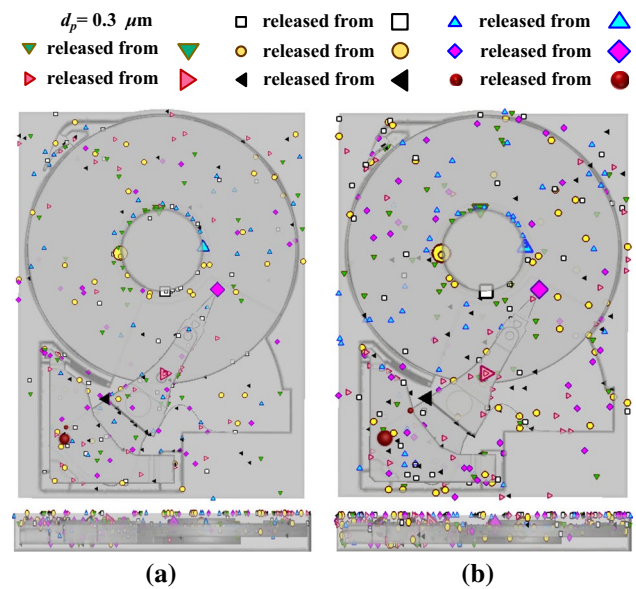


Fig. 5 Trapping status for Al₂O₃ particles released from different positions inside the air-filled drive

motor is a major heat generation component. And the other reason is that the low-speed flow at the ID results in a low forced convection heat transfer coefficient. In addition, temperature gradients of dT/dx and dT/dy inside the air-filled drive are larger than those inside the helium-filled drive.

Table 3 Particle trapping rate at 5400 RPM inside the air-filled drive

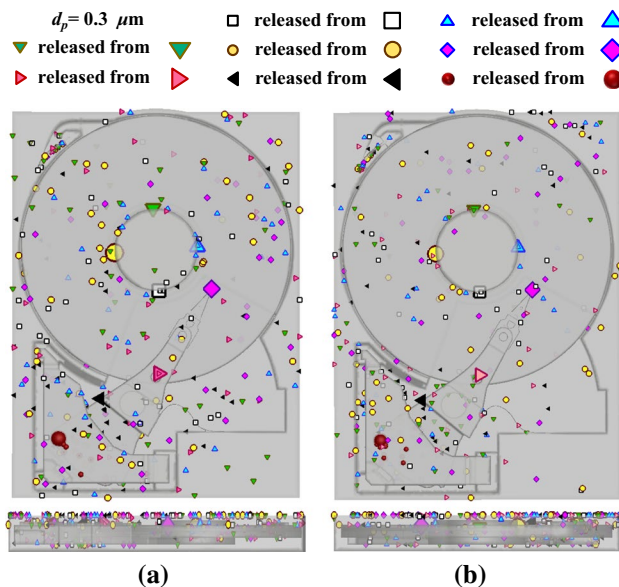
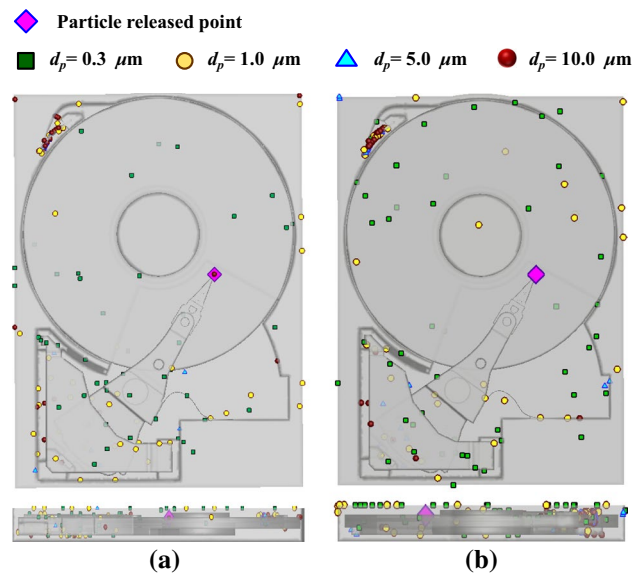
HDD component	Release position ($d_p = 0.3 \mu\text{m}$)			
	ID	MD	OD	VCM region
Particle trapping rate (%)				
Without considering the temperature				
Cover	20	33	36	21
Base	18	19	15	23
Arm and HGA	9	6	13	10
Bobbin and magnet	11	16	16	19
Disk	38	22	17	22
Filter	4	4	3	5
Considering the temperature				
Cover	34	38	30	28
Base	16	16	13	23
Arm and HGA	9	9	21	13
Bobbin and magnet	15	17	24	17
Disk	23	18	10	16
Filter	3	2	2	3

Table 4 Particle trapping rate at 5400 RPM inside the helium-filled drive

HDD component	Release position ($d_p = 0.3 \mu\text{m}$)			
	ID	MD	OD	VCM region
Particle trapping rate (%)				
Without considering the temperature				
Cover	31	30	33	26
Base	12	24	15	16
Arm and HGA	9	8	8	19
Bobbin and magnet	20	21	21	25
Disk	20	12	14	11
Filter	8	5	9	3
Considering the temperature				
Cover	36	33	31	29
Base	19	22	21	21
Arm and HGA	6	12	10	11
Bobbin and magnet	23	19	21	21
Disk	13	10	13	10
Filter	3	4	4	8

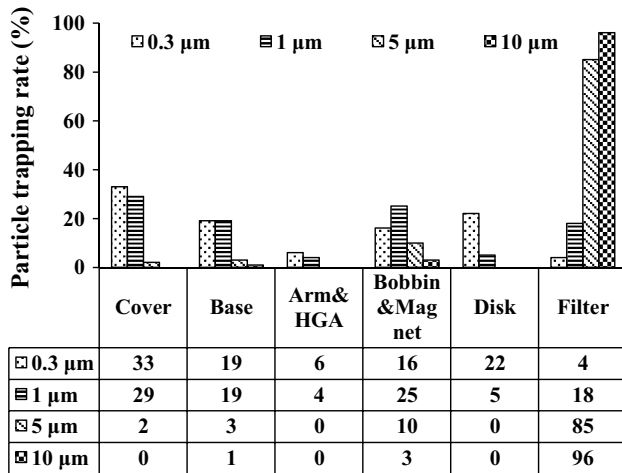
3.2 Different particle release positions

Fifty Al_2O_3 particles with a diameter of $d_p = 0.3 \mu\text{m}$ are released from eight release positions as shown in Fig. 5. Eight big symbols represent eight release positions. Four of them are located at the ID on the disk surface. The rest four release positions are at the HGA tip (above the MD of the disk), the center of the arm (above the OD of the disk), and

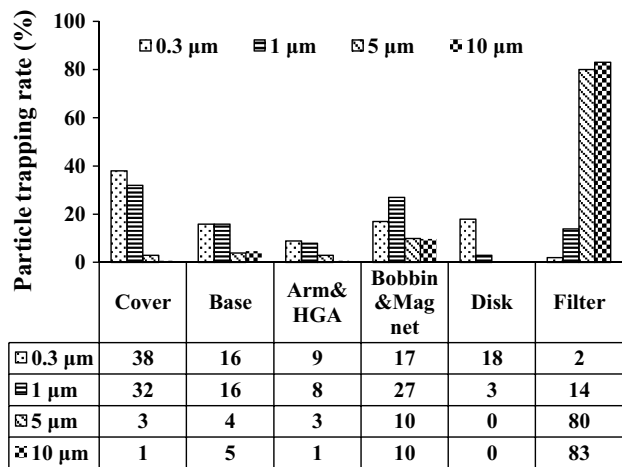
**Fig. 6** Temperature effects on the trapping status for Al_2O_3 particles released from different positions inside the helium-filled drive**Fig. 7** Temperature effects on the trapping status for Al_2O_3 particles of various sizes inside the air-filled drive

VCM region, respectively. Small symbols represent final positions of particles, where particles are trapped.

Figure 5 shows the trapping status for Al_2O_3 particles inside the air-filled drive. It is shown in Table 3 that over one-third of particles are trapped by the inner edge of the disk when particles released from the ID when not considering the temperature. This can be explained by that the velocity of the air flow near the spindle is low. The velocity of particles involved in this air flow is smaller than the



(a)



(b)

Fig. 8 Particle trapping rate for various particles sizes when particles are released from the MD inside the air-filled drive

critical velocity of the disk surface, so particles are trapped immediately after released. In addition, for four investigated particle release positions as listed in Table 3, the number of particles trapped by the disk decreases after considering the temperature. The reason behind this is that the temperature gradient near the disk surface, especially near the ID mentioned above, results in the thermophoretic force acting on the particle which moves away from the disk.

Figure 6 shows the trapping status for Al₂O₃ particles inside the helium-filled drive. From a comparison of the particle trapping rate in Tables 3 and 4, it can be found that the number of particles trapped by the disk inside the air-filled drive is significantly more than that inside the helium-filled drive when not considering the temperature. The possible reason for this difference is that the air flow velocity has a large perturbation. Therefore, particles involved in the turbulent air flow have more chance to attach onto the

disk surface. After considering the temperature, the particle trapping rate by the disk decreases both inside the air-filled drive and the helium-filled drive. And its reduction inside the air-filled drive is larger. Especially, inside the air-filled drive as particles released from the ID, the trapping rate decreases from 38 to 23%, while the decrease is 7% (from 20 to 13%) inside the helium-filled drive. This may be also explained by that the temperature gradient near the ID inside the air-filled drive is significantly larger than that inside the helium-filled drive mentioned above. Therefore, particles in the air flow are subjected to a bigger thermophoretic force and more easily move away from the disk surface.

3.3 Different particle sizes

Fifty Al₂O₃ particles ($d_p = 0.3, 1, 5$ and $10 \mu\text{m}$) are released from the HGA tip (above the MD of the disk) as shown in Fig. 7. Corresponding particle trapping rate inside the air-filled drive are tabulated in Fig. 8. It can be seen that the smaller the particle diameter, the more the particle trapping rate by the cover increases after considering the temperature. It means that the thermophoretic force has a great influence on trajectories of submicron particles. In addition, the number of particles trapped by the filter decreases after considering the temperature. Therefore, the filter cannot provide the expected filtration efficiency for particles in a high temperature environment. Moreover, when the particle diameter exceeds $5 \mu\text{m}$, there are no particles trapped by the disk regardless of whether the temperature is considered or not. It indicates that small particles will

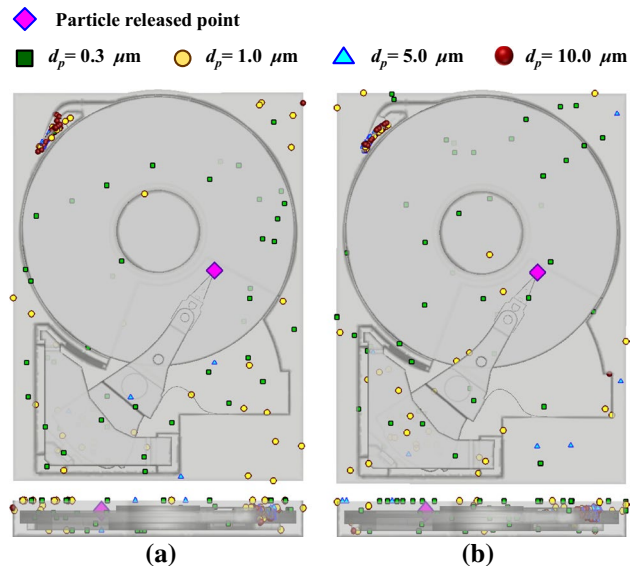


Fig. 9 Temperature effects on the trapping status for Al₂O₃ particles of various sizes inside the helium-filled drive

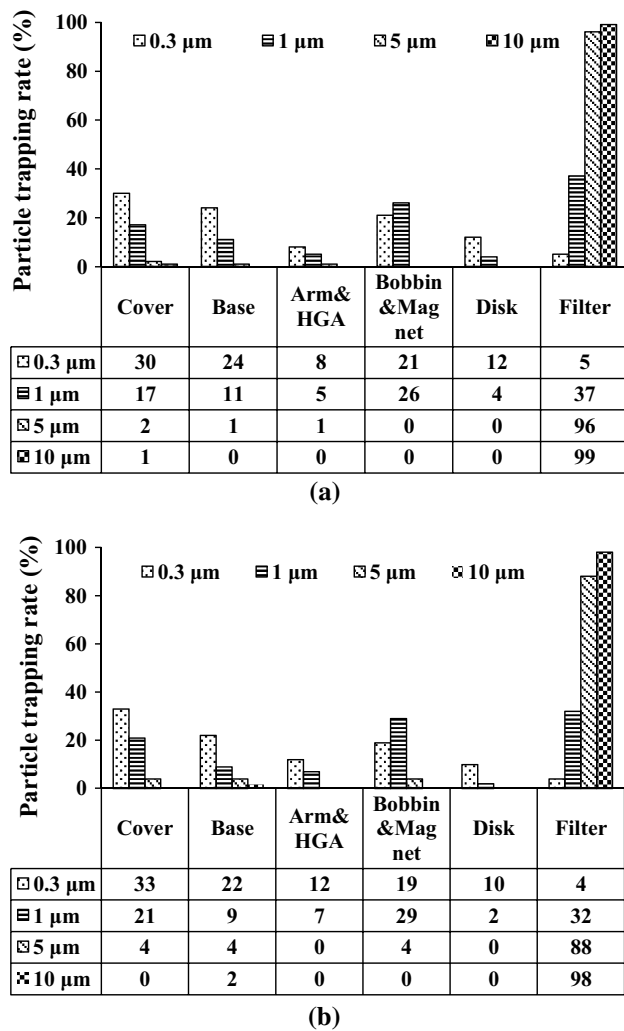


Fig. 10 Particle trapping rate for various particles sizes when particles are released from the MD inside the helium-filled drive

more likely degrade the HDI reliability since they can follow the rotatory flow well and have more chance to collide with the disk surface, and then easily attach onto the disk surface. Furthermore, when the particle diameter exceeds 1 μm , the number of particles trapped by the filter dramatically increases. This is because the big particle has a large inertia after being accelerated by the high rotational speed air flow, and then overcomes the centripetal force and flies to the filter.

The particle trapping status and trapping rate inside the helium-filled drive are shown in Figs. 9 and 10, respectively. Compared Figs. 8 and 10, it can be found that the number of particles trapped by the disk inside the helium-filled drive is significantly less than that inside the air-filled drive. It means that particles inside the air-filled drive will more likely degrade the HDI reliability.

4 Summary

In this paper, Al_2O_3 particle trajectories inside 2.5 inch air-filled drives and helium-filled drives are investigated by considering major heat sources such as the spindle motor and VCM, and trapping criterions. Results observed are as follow:

1. The helium-filled drive has more heat stability than the air-filled drive. The velocity along the vertical direction inside the helium-filled drive changes more smoothly compared inside the air-filled drive.
2. After considering the temperature, the particle trapping rate by the disk decreases both inside the air-filled drive and the helium-filled drive. And its reduction inside the air-filled drive is larger.
3. Small particles will more likely degrade the HDI reliability since they can follow the rotatory flow well and have more chance to collide with the disk surface, and then easily attach onto the disk surface.
4. Particles in the air-filled drive will more likely degrade the HDI reliability since they can easily attach onto the disk surface compared to the helium-filled drive.

Although there is a great improvement in present work for investigating temperature effects on particles trajectories, it ignores collisions among particles as well as the secondary movement of particles induced by the shear flow inside the drive. Also, effects of the arm swing are not considered. Our next work will perform a further study of particle trajectories.

Acknowledgements This work is supported by National Natural Science Foundation of China (Grant No. 51505342), the Fundamental Research Funds for the Central Universities of China (Grant No. 2042015kf0193), and the scholarship from China Scholarship Council (CSC) under the Grant CSC No. 201606275004. Authors gratefully acknowledge all the support.

References

- Cui FH, Li H, Shen SN, Liu S, Wu SJ (2016) Simulation of air flow and particle trajectories in the head–disk interface. *IEEE Trans Magn*. 52:3301905
- Dahneke B (1971) The capture of aerosol particles by surfaces. *J Colloid Interface Sci* 37:342–353
- Liu NY, He ZM, Chow CKT, Loh HT (2011) A Numerical investigation of particle trajectory inside hard disk drives. *IEEE Trans Magn* 47:1890–1892
- Liu NY, Zhang QD, Sundaravadivelu K (2013) A numerical simulation of particle trajectory in thin hard disk drive. *IEEE Trans Magn* 49:2590–2593
- Liu S, Li H, Shen SN, Wu SJ (2015) Simulation of particle trajectory in the head–disk interface. *IEEE Trans Magn* 51:3301404

- Liu S, Li H, Shen SN, Wu SJ (2016) Simulation of particle rebounding from the slider air bearing surface. *Microsyst Technol* 22:1475–1481
- Ng EYK, Liu NY, Tan YCM (2011) Structure optimization study of hard disk drives to reduce flow-induced vibration. *Open Numer Methods J* 3:31–41
- Stratmann F, Fissan H, Papperger A, Friedlander S (1988) Suppression of particle deposition to surfaces by the thermophoretic force. *Aerosol Sci Technol* 9:115–121
- Tan CP, Yip TH, Tan DTD (2011) Thermal characteristics of enterprise-class hard disk drives. *IEEE Trans Magn* 1:868–872
- Yang JP, Tan CP, Ong EH (2010) Thermal analysis of helium-filled enterprise disk drive. *Microsyst Technol* 16:1699–1704
- Zhang GQ, Zhu YW, Li H, Shen SN, Yang Y, Liu S, Lei X, Wu SJ (2016a) Simulation of particle trajectory in the hard disk drive considering the trapping criterion. *IEEE Trans Magn* 52:3001806
- Zhang GQ, Li H, Shen SN, Wu SJ (2016b) Simulation of HGA vibration characteristics inside the helium-filled hard disk drive. *IEEE Trans Magn* 52:3300806
- Zhang GQ, Yang Y, Li H, Shen SN, Wu SJ (2016c) Suppressing flow-induced vibration of HGA by an acoustic PZT actuator in hard disk drives. *Microsyst Technol* 22:1467–1474
- Zhang GQ, Li H, Shen SN, Zheng H, Lei J, Wu SJ (2016d) Simulation of temperature around laser-heating media in heat-assisted magnetic recording. *Microsyst Technol* 22:2877–2882